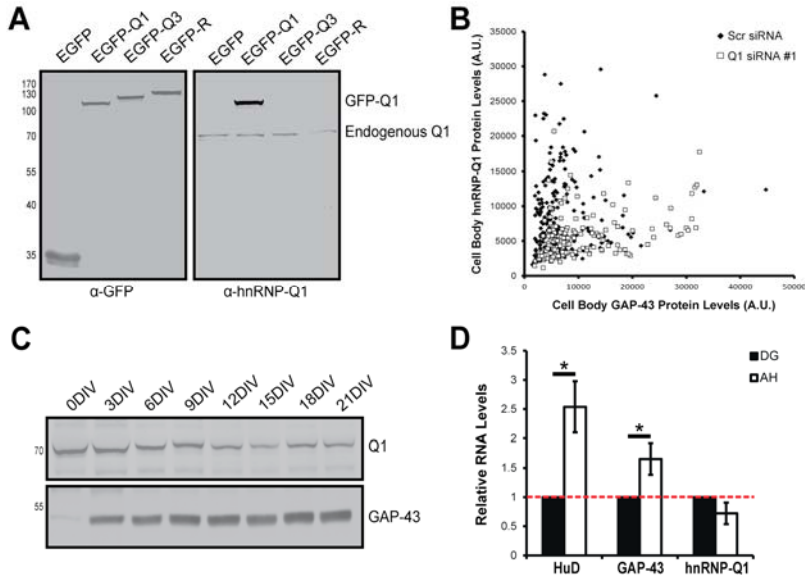


# Supplemental Materials

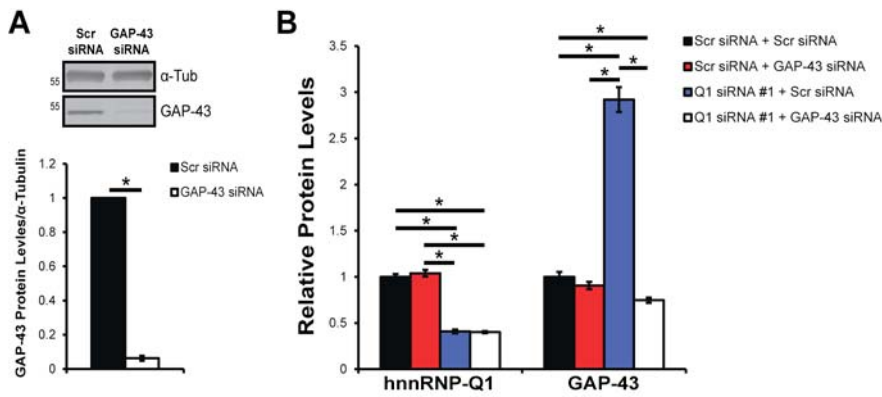
*Molecular Biology of the Cell*

Williams et al.

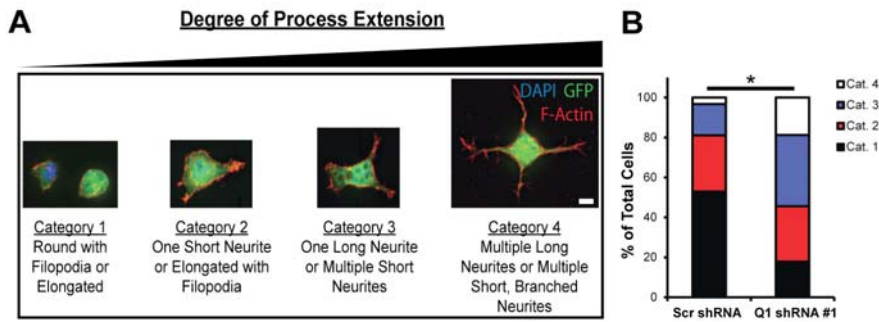
## Supplemental Material



**Supplemental Figure 1.** (A) EGFP and EGFP-tagged hnRNP-Q1 and the homologous proteins hnRNP-Q3 and hnRNP-R were overexpressed in N2a cells for ~16 hours and lysates were immunoblotted for GFP and hnRNP-Q1. (B) Plot of cell body hnRNP-Q1 protein levels against cell body GAP-43 protein levels for each cell from Figure 1, C-G. (C) Time course of high-density cultured primary cortical neurons immunoblotted for hnRNP-Q1 and GAP-43. (DIV = days *in vitro*) (D) The levels of *HuD*, *Gap-43* and *hnRNP-Q1* mRNAs in Ammon's Horn (AH) and the Dentate Gyrus (DG) were quantified by qRT-PCR. The relative level of each mRNA in Ammon's Horn is shown relative to the Dentate Gyrus. n=4, t-test, p-values: *HuD* p=0.0261, *GAP-43* p=0.0330, *Q1* p=0.1006.



**Supplemental Figure 2.**(A) N2a cells were transfected with GAP-43 or Scrambled siRNA and immunoblotted for GAP-43 and  $\alpha$ -Tubulin after 72 hours.  $n=7$ , one-sample t-test,  $p$ -value $<0.0001$ . (B) Primary cortical neurons were transfected with hnRNP-Q1 #1 or Scrambled siRNA, GAP-43 or Scrambled siRNA and Lifeact-GFP by nucleofection and processed for immunofluorescence with GAP-43 and hnRNP-Q1 antibodies after 28.5 hours. Cell body intensity of GAP-43 and hnRNP-Q1 of selected cells from Figures 2 and 3 were quantified.  $n=7$ , Scr + Scr: 62 out of 173 cells, Scr + GAP-43: 59 out of 181 cells, Q1 + Scr: 47 out of 170 cells and Q1 + GAP-43: 145 out of 184 cells from 7 independent experiments, one-way ANOVA, Tukey's post-hoc, hnRNP-Q1  $p$ -values: Scr + Scr vs. Scr + GAP-43  $p=0.6221$ , Scr + Scr vs Q1 + Scr  $p<0.0001$ , Scr + Scr vs Q1 + GAP-43  $p<0.0001$ , Scr + GAP-43 vs Q1 + Scr  $p<0.0001$ , Scr + GAP-43 vs Q1 + GAP-43  $p<0.0001$ , Q1 + Scr vs Q1 + GAP-43  $p=0.9958$ , GAP-43  $p$ -values: Scr + Scr vs. Scr + GAP-43  $p=0.716$ , Scr + Scr vs Q1 + Scr  $p<0.0001$ , Scr + Scr vs Q1 + GAP-43  $p=0.0037$ , Scr + GAP-43 vs Q1 + Scr  $p<0.0001$ , Scr + GAP-43 vs Q1 + GAP-43  $p=0.1436$ , Q1 + Scr vs Q1 + GAP-43  $p<0.0001$ .



**Supplemental Figure 3.** (A) N2a cells were transfected with hnRNP-Q1 #1 or Scrambled shRNA, which co-expresses GFP. The cells were fixed after 72 hours and processed for immunofluorescence with fluorescently conjugated phalloidin to label F-actin. Transfected cells were selected by GFP signal and representative images from each category were assembled. Scale bar = 10 $\mu$ m. (B) N2a cells were transfected with hnRNP-Q1 #1 or Scrambled shRNA and processed for immunofluorescence with GAP-43 and hnRNP-Q1 antibodies after 72 hours. Cells were then imaged and categorized based on their degree of process extension. Percent of cells in each category: Scr: Cat. 1 = 52.9%, Cat 2. = 28.2%, Cat 3. = 15.7%, Cat. 4 = 3.2%, Q1: Cat. 1 = 17.8%, Cat 2. = 27.7%, Cat 3. = 35.7%, Cat. 4 = 18.8%, n=4, Scr: 433 cells and Q1: 314 cells from 4 independent experiments, Mann-Whitney test, p-value<0.0001.

**A**Ms *Gap-43* mRNA

Position	Region	Sequence	G-Score
14	5'-UTR	<u>GGGAGGGA</u> <u>GGGAGGG</u>	42
88	5'-UTR	<u>GGGAAUAA</u> <u>GG</u> <u>AAGAGA</u> <u>GG</u> <u>AGGAAAGG</u>	21
338	Coding	<u>GG</u> <u>CCGAGG</u> <u>CCAA</u> <u>GG</u> <u>AGAA</u> <u>GG</u>	21
482	Coding	<u>GG</u> <u>AGAAGA</u> <u>GG</u> <u>GUGAAG</u> <u>GG</u> <u>GAUGC</u> <u>GG</u>	19
76	5'-UTR	<u>GGUGG</u> <u>AGAGGGG</u>	18
120	5'-UTR	<u>GGCA</u> <u>GG</u> <u>AAGA</u> <u>GG</u> <u>CA</u> <u>GG</u>	18
518	Coding	<u>GG</u> <u>AAAA</u> <u>GG</u> <u>CC</u> <u>GG</u> <u>CUCAG</u> <u>CGG</u>	17
378	Coding	<u>GG</u> <u>UGUG</u> <u>GAGA</u> <u>AGAA</u> <u>GG</u> <u>AGGG</u>	16
443	Coding	<u>GG</u> <u>CUGA</u> <u>GG</u> <u>AGCC</u> <u>CAGCA</u> <u>GG</u> <u>CA</u> <u>GG</u>	13
587	Coding	<u>GG</u> <u>CUGA</u> <u>AAGAU</u> <u>GG</u> <u>CCC</u> <u>AGCCAA</u> <u>GG</u> <u>AGG</u>	13

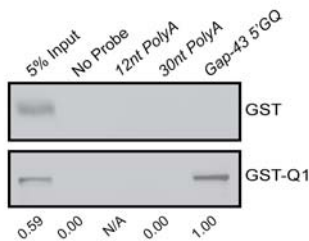
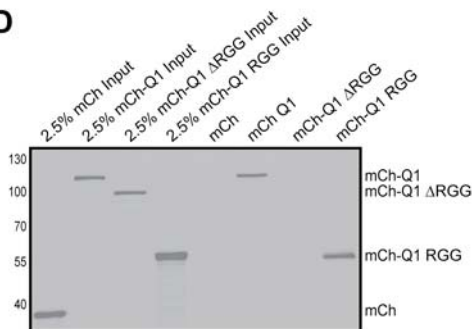
**B**Hu *Gap-43* mRNA

Position	Region	Sequence	G-Score
239	5'-UTR	<u>GGGAGAGAGAG</u> <u>GGGAGGGAGGG</u>	36
73	5'-UTR	<u>GGGGGGAA</u> <u>GG</u> <u>AGAAAAAA</u> <u>GG</u> <u>AGAAGAGAGG</u>	19
311	5'-UTR	<u>GGUGGAGAG</u> <u>GGGGGG</u>	19
357	5'-UTR	<u>GGCA</u> <u>GG</u> <u>AAGAA</u> <u>GG</u> <u>CAAG</u> <u>GG</u>	18
1011	Coding	<u>GGGGUGG</u> <u>GAGA</u> <u>AGAA</u> <u>GGG</u> <u>GAGA</u> <u>AGG</u>	17
1451	Coding	<u>GGACGAG</u> <u>GGU</u> <u>AAAGA</u> <u>AGAGG</u> <u>GAACCUGA</u> <u>GG</u>	17
1112	Coding	<u>GG</u> <u>AGAAGA</u> <u>GGGGG</u> <u>AGG</u>	15
1160	Coding	<u>GGCUCCTGCAUCCUCAGAGG</u> <u>AGAA</u> <u>GGCCGG</u>	7

**C****RNA Probe Sequences**

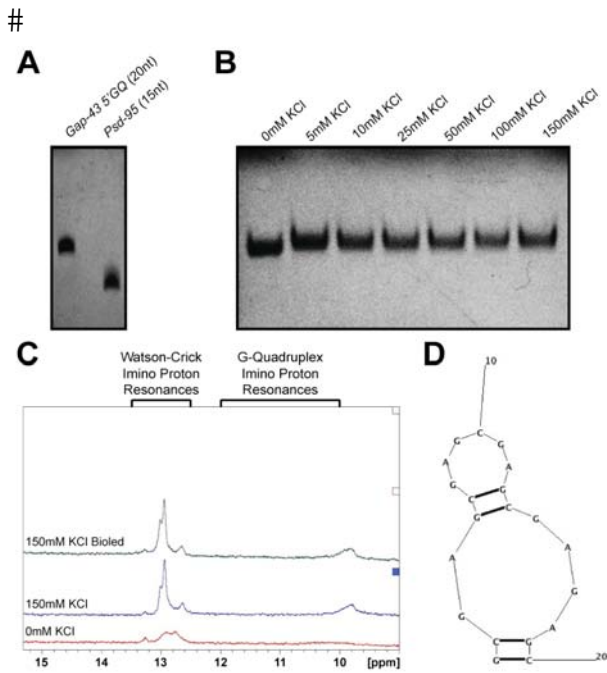
12nt PolyA: 5'-Biotin-AAAAAAAAAAAA-3'

30nt PolyA: 5'-Biotin-AAAAAAAAAAAAAAAAAAAAAAAAAAAA-3'

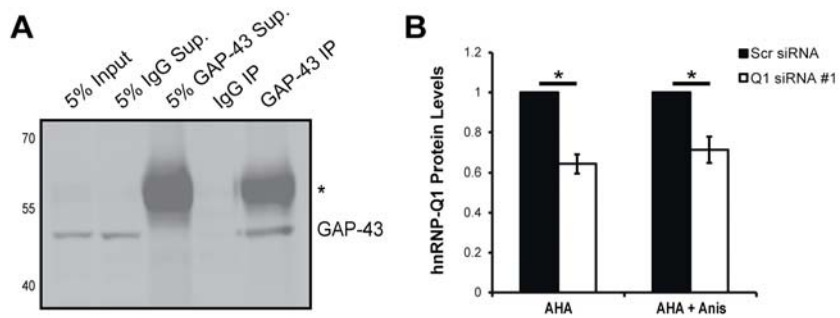
*Gap-43* 5'GQ: 5'-Biotin-GGGAGGGAGGGAGGGAGAGC-3'**D**

**Supplemental Figure 4.** Predicted GQs in (A) mouse and (B) human *Gap-43* mRNA. Red underlined nucleotides are predicted to be involved in GQ structure formation. QGRS Mapper software was used for the prediction (Kikin et al., 2006). (C) 5' biotin end labeled *Gap-43* 5'GQ, 12 nucleotide poly(A) and 30 nucleotide poly(A) RNA probes were incubated with recombinant GST or GST-hnRNP-Q1 protein and precipitated with NeutrAvidin beads. Co-purified protein was assessed by GST immunoblot and relative band intensity is listed below the immunoblot. (D) 5' biotin end labeled *Gap-43* 5'GQ RNA probe was incubated with N2a cell lysates that were transfected with 3x-Flag-mCherry, 3x-Flag-mCherry-hnRNP-Q1, 3x-Flag-mCherry-hnRNP-Q1

$\Delta$ RRG Box or 3x-Flag-mCherry-hnRNP-Q1 RGG Box ~16 hours prior to lysing. The 5'GQ probe was precipitated with NeutrAvidin beads and co-purified protein was assessed by Flag immunoblot.

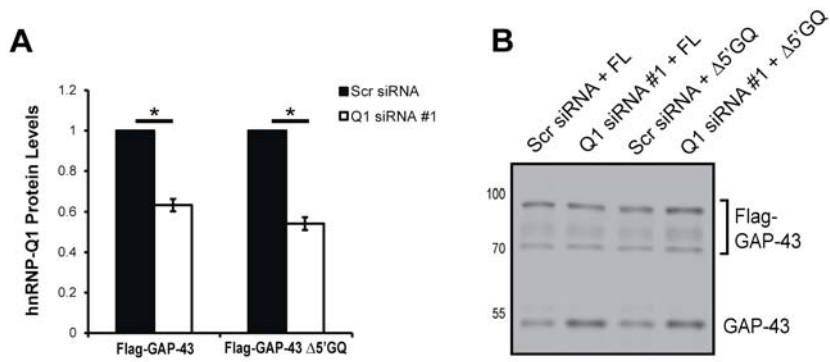


**Supplemental Figure 5.** (A) The purity of the *Gap-43* 5'GQ RNA probe was assessed by denaturing polyacrylamide gel electrophoresis. A PSD-95 RNA probe was run for comparison. (B) The *Gap-43* 5'GQ RNA probe was annealed in increasing KCl concentrations and GQ conformation was assessed by native gel electrophoresis. (C) 1D  $^1\text{H}$  NMR spectroscopy with the mutant *Gap-43* 5'GQ RNA probe revealed that imino proton resonances are not present in the 10-12 ppm region demonstrating that mutation of guanine residues that are involved in GQ formation prevents the structure from forming. Imino proton resonances are present in the 12.6-13.4 ppm region, which correspond to Watson-Crick G-C base pairs. (D) The mutant *Gap-43* 5'GQ RNA probe is predicted to form a hairpin structure, which is supported by the 1D  $^1\text{H}$  NMR spectroscopy results.



**Supplemental Figure 6.** (A) Endogenous GAP-43 protein was immunoprecipitated from N2a cell lysates and immunoprecipitation efficiency was assessed by immunoblot for GAP-43. Sup. = supernatant, \* = non-specific bands. (B) hnRNP-Q1 knockdown efficiency for endogenous AHA experiments in Figure 7, A-C. n=3, one-sample t-test, p-values: AHA p=0.0161, AHA + Anis p=0.0489.





**Supplemental Figure 7.**(A) hnRNP-Q1 knockdown efficiency for reporter AHA experiments in Figure 8, A and B.  $n=6$ , one-sample t-test, p-values: Flag-GAP-43  $p<0.0001$ , Flag-GAP-43  $\Delta$ GQ  $p<0.0001$ . (B) Representative example of Flag-GAP-43 and Flag-GAP-43  $\Delta$ GQ construct overexpression for reporter AHA experiments (3xFlag-mCherry-GAP-43 predicted to be  $\sim 75$  kDa).